Reciprocal regulation of airway rejection by the inducible gas-forming enzymes heme oxygenase and nitric oxide synthase

Kanji Minamoto,[1] Hiroaki Harada,[2] Vibha N. Lama,[3] Maksim A. Fedarau,[2] and David J. Pinsky[2]

[1]Department of Surgery, Kagawa Prefectural Central Hospital, Takamatsu, Kagawa 760-8557, Japan
[2]Division of Cardiology and [3]Division of Pulmonary and Critical Care Medicine, Department of Internal Medicine, University of Michigan Cardiovascular Center, Ann Arbor, MI 48109

Obliterative bronchiolitis (OB) develops insidiously in nearly half of all lung transplant recipients. Although typically preceded by a $CD8^+$ T cell–rich lymphocytic bronchitis, it remains unresponsive to conventional immunosuppression. Using an airflow permissive model to study the role of gases flowing over the transplanted airway, it is shown that prolonged inhalation of sublethal doses of carbon monoxide (CO), but not nitric oxide (NO), obliterate the appearance of the obstructive airway lesion. Induction of the enzyme responsible for the synthesis of CO, heme oxygenase (Hmox) 1, increased carboxyhemoglobin levels and suppressed lymphocytic bronchitis and airway luminal occlusion after transplantation. In contrast, zinc protoporphyrin IX, a competitive inhibitor of Hmox, increased airway luminal occlusion. Compared with wild-type allografts, expression of inducible NO synthase (iNOS), which promotes the influx of cytoeffector leukocytes and airway graft rejection, was strikingly reduced by either enhanced expression of Hmox-1 or exogenous CO. Hmox-1/CO decreased nuclear factor (NF)-κB binding activity to the iNOS promoter region and iNOS expression. Inhibition of soluble guanylate cyclase did not interfere with the ability of CO to suppress OB, implicating a cyclic guanosine 3′,5′-monophosphate–independent mechanism through which CO suppresses NF-κB, iNOS transcription, and OB. Prolonged CO inhalation represents a new immunosuppresive strategy to prevent OB.

CORRESPONDENCE
David J. Pinsky:
dpinsky@umich.edu

Abbreviations used: COHb, carboxyhemoglobin; CoPP; cobalt protoporphyrin IX; EMSA, electrophoretic mobility shift assay; Hmox, heme oxygenase; iNOS, inducible NO synthase; L-NIL, N^6-(1-iminoethyl)-L-lysine dihydrochloride; OB, obliterative bronchiolitis; ODQ, 1H-[1,2,4]oxadiazolo[4,3, -a] quinoxalin-1-one; sGC, soluble guanylate cyclase; ZnPP, zinc protoporphyrin IX.

Lung transplantation across an allogeneic barrier often provokes a severe inflammatory response, characterized by a massive lymphocytic influx into the graft. Although vascular structures can be targets of chronic rejection, as in all transplanted solid organs, the pronounced involvement of airway structures represents a unique and clinically devastating feature in chronically rejecting transplanted lungs (1). The transplanted airway resides in a unique topographic interface and is subjected to the continuous topical exposure of biological gases both produced within the organism and inhaled from the external environment. Synthesis of NO, a diatomic gas with pleiotropic immune and nonimmune functions, is increased during airway rejection, where it has been shown to exacerbate lymphocytic bronchitis and airway obliteration (2). Expression of the inducible heme oxygenase (Hmox) enzyme responsible for synthesis of a related diatomic gas, CO, is also increased in human lung transplants with acute cellular rejection and obliterative bronchiolitis (OB; reference 3). In contrast to the activity of inducible NO synthase (iNOS) as a potent immune effector mechanism, Hmox-1 has been shown to possess antiinflammatory properties. As heme oxygenases are the rate-limiting enzymes (4, 5) in the synthesis of the endogenous gaseous molecule CO as a byproduct of heme catabolism, it has been suggested that CO derived from this catalytic process may have important antiinflammatory functions (6, 7). The strong induction of Hmox during lung transplant rejection leads to the hypothesis that endogenous expression of Hmox-1 and derivative CO may serve as countervailing mechanisms to limit tissue inflammation and injury induced by iNOS in the setting of airway transplant rejection.

K. Minamoto and H. Harada contributed equally to this work.
K. Minamoto's present address is Cancer and Thoracic Surgery, Okayama University Graduate School of Medicine and Dentistry, Okayama City 700-8558, Japan.

The Journal of Experimental Medicine

To test this hypothesis, a new model of transplantation-associated obliterative airway disease was studied in mice lacking the *Hmox-1* gene, or those in which Hmox-1 expression was enhanced. Mice were subjected to prolonged inhalation of either CO or NO in the presence or absence of various pharmacological inhibitors of downstream signaling cascades. Data reveal that endogenous Hmox-1 expression/CO production provide critical and counterbalancing protection against the OB induced by enhanced iNOS expression in the airway allografts. Additional data suggest that suppression of NF-κB nuclear translocation by CO results in down-regulation of iNOS expression and consequent suppression of OB development.

RESULTS

Morphometric analysis of graft narrowing

Airway transplantation across an allogeneic barrier in an airflow-permissive transplant model results in significant luminal narrowing, which is not seen in the same model when the transplanted graft is isogeneic with the recipient. Characteristic thickening of the epithelial and subepithelial layers lead to partial concentric graft luminal occlusion (47 ± 4% for wild-type allografts vs. 16 ± 1% for isografts; $P < 0.05$; Fig. 1). To determine whether induction of Hmox-1 can alter this natural history, cobalt protoporphyrin IX (CoPP) was administered to donors and recipients. This treatment regimen was associated with a strong induction of Hmox-1 protein (see Fig. 3 i and Fig. 4 C) and mRNA (see Fig. 4 A) in the transplanted grafts. CoPP treatment significantly reduced luminal occlusion ($P < 0.05$; Fig. 1). In contrast to CoPP, treatment with zinc protoporphyrin IX (ZnPP), which acts as a competitive inhibitor of Hmox activity, resulted in a substantial amount of luminal occlusion (50 ± 2%). Preliminary experiments indicated that carboxyhemoglobin (COHb) levels were 17 ± 1% in mice ($n = 5$) exposed to 250 ppm CO for 2 wk. When Hmox-$1^{+/+}$ allograft recipients were placed in a similar (250 ppm) CO-rich environment for 2 wk after transplantation, graft luminal occlusion was diminished to a similar degree as that seen after Hmox-1 induction with CoPP. The suppressive effect of CO on airway luminal obliteration was not seen when CO was given solely to the donor animal for 24 h before the tracheal harvest (see Fig. 2 C).

To further evaluate the role of endogenous expression on graft luminal obliteration, the next series of experiments was performed using donor trachea, from mice lacking the *Hmox-1* gene, transplanted into allogeneic Hmox-$1^{+/+}$ recipients. In these experiments, a significant increase in luminal occlusion was observed (69 ± 6%) compared with that seen in Hmox-$1^{+/+}$ to Hmox-$1^{+/+}$ allotransplants (47 ± 4%; $P < 0.05$). Inhalation of 250 ppm CO for 2 wk significantly rescued the Hmox-1–null transplants from the devel-

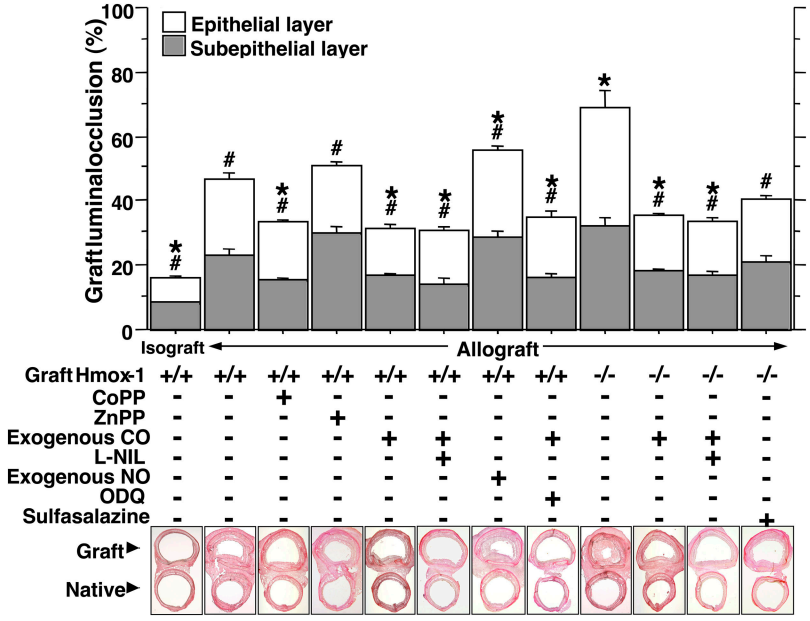

Figure 1. Graft luminal narrowing at 3 wk after transplantation. Representative sections and morphometric analysis of sections for each of the indicated conditions are shown. Allograft recipients were all Hmox-$1^{+/+}$; donor tracheas were obtained from either Hmox-$1^{+/+}$ or Hmox-$1^{-/-}$ mice as indicated in the figure. Hmox-$1^{+/+}$ isografts are shown for comparison. The following conditions were examined: an Hmox-1–inducer (CoPP); an Hmox-inhibitor (ZnPP); exogenous CO (250 ppm) or NO (20 ppm) inhalation for 2 wk after transplantation; and pharmacological inhibitors (L-NIL to inhibit iNOS or ODQ to inhibit sGC). For certain experiments, sulfasalazine, a specific inhibitor of NF-κB (references 36, 37), was given to Hmox$^{-/-}$ graft–recipient mice as a drinking water supplement (130 mg/kg/d) for 3 wk after transplantation. 5–10 transplants were performed for each group. *, $P < 0.05$ versus Hmox-$1^{+/+}$; #, $P < 0.05$ versus Hmox-$1^{-/-}$ allografts. Representative histological sections are shown under each bar. Data are mean ± SEM.

opment of airway luminal obliteration (35 ± 2%; $P < 0.05$ vs. Hmox-$1^{-/-}$ allografts in the absence of inhaled CO).

In a recent study using the identical airway transplant model system, induction of iNOS was shown to be a pathological mediator of airway rejection, the blockade of which could reduce airway luminal obliteration (2). In the current experiments, coadministration of the iNOS blocker N^6-(1-iminoethyl)-L-lysine dihydrochloride (L-NIL) with inhaled CO (in either Hmox-$1^{-/-}$ or Hmox-$1^{+/+}$ transplants) did not further reduce luminal obliteration compared with conditions in which CO was administered alone (Fig. 1). When inhaled NO was administered to Hmox-$1^{+/+}$ allograft recipients at a dose that results in comparable soluble guanylate cyclase (sGC) activation (20 ppm; reference 8) for 2 wk after transplantation, it became clear that prolonged NO exposure not only did not reduce luminal obliteration but actually exacerbated it (56 ± 3%; $P < 0.05$ vs. Hmox-$1^{+/+}$ allografts). This is in stark contrast to the beneficial vascular effects of inhaled NO seen shortly after lung transplantation (9). Collectively, these data indicate that NO and CO have distinct biological profiles in this allograft model of OB. To test the mechanistic link between Hmox-1, CO, and iNOS induction, we studied whether inhibition of NOS2 (iNOS) activity might abrogate luminal obliteration, particularly in Hmox-1–null allografts (Fig. 2 A). In a completely distinct cohort of animals from those shown in Fig. 1 A, isografts or allografts were implanted and luminal obliteration assessed at 1 wk without immunosuppression. L-NIL brought luminal obliteration in Hmox-$1^{-/-}$ mice down to the baseline levels seen in Hmox-$1^{+/+}$ allografts. The overall diminution of luminal obliteration in WT allografts is similar to that which we have previously observed (2).

The next question, which was experimentally addressed, was whether the site of Hmox-1 expression was important in the observed protection against luminal narrowing. This question is particularly relevant because iNOS expressed in airway graft tissue has no apparent effect on airway rejection, whereas recipient leukocyte-derived iNOS plays a critical exacerbating role (2). The situation appears to be quite dif-

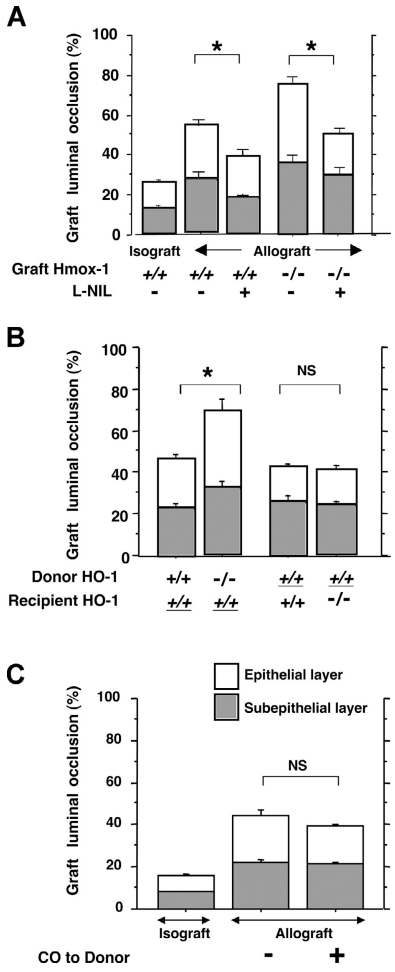

Figure 2. Graft luminal occlusion in response to the presence/absence of the *Hmox-1* gene, with or without iNOS inhibition or donor-inhaled CO. (A) Effect of iNOS inhibition in the recipient (5mg/kg/d L-NIL) on graft luminal occlusion. Six transplants were performed for each experiment. *, $P < 0.05$. (B) Effect of epithelial- versus leukocyte-derived Hmox-1 (HO-1) on graft luminal narrowing. Genotypes of donors and recipients were either Hmox-$1^{+/+}$ or Hmox-$1^{-/-}$, as indicated. Genotypes that are underlined represent the B10.A strain background, whereas those that are not underlined represent the 129Sv × BALB/c strain background. Note that the leftmost two bars present the same data as are shown in A, repeated here to facilitate comparison (*, $P < 0.05$; $n = 8$ for the right and rightmost bars). (C) Effect of a 250-ppm CO dose for 24 h given solely to donor mice before the airway transplantation. The number of transplants performed for each experiment were as follows: 4 (left), 11 (middle), and 5 (right). Data are mean ± SEM.

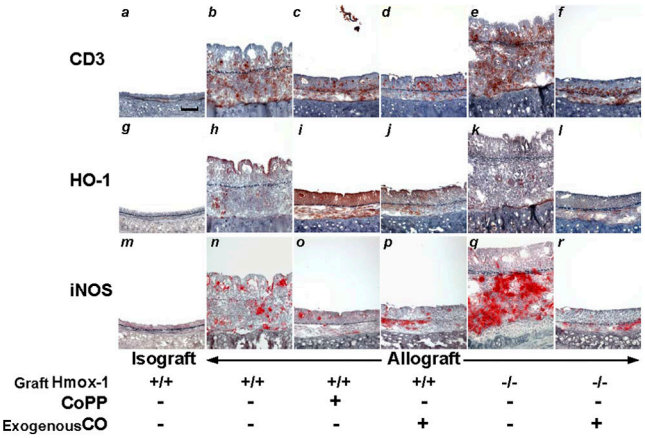

Figure 3. Immunohistochemical detection of graft-infiltrating T cells and the enzymes Hmox-1 and iNOS. Immunohistochemical staining of the pan–T cell marker CD3 (a–f, brown), as well as Hmox-1 (HO-1; g–l, brown) and iNOS (m–r, red), in adjacent serial sections from airway grafts at 3 wk after transplantation. Most graft-infiltrating cells are detected as $CD3^+$ T lymphocytes. Hmox-1 expression is mainly localized at epithelial cells in Hmox-$1^{+/+}$ allografts and is overexpressed after CoPP treatment. Some cells expressing iNOS are recognized as $CD3^+$ T lymphocytes. The donor Hmox-1 genotype and treatment regimen are indicated. The conditions shown are described in the legend to Fig. 1. Bar, 50 μm.

ferent for Hmox-1, in that Hmox expression in the graft, rather than in the recipient, dominates the course of rejection. Exacerbation of the airway occlusive lesions was observed when the grafts themselves lacked the *Hmox-1* gene; however, lesions were not exacerbated when the graft tissue expressed Hmox-1, but circulating recipient cells were Hmox-1 null (Fig. 2 B). These differences could not be accounted for by differences in the background strain because graft luminal narrowing for Hmox-$1^{+/+}$ trachea transplanted into Hmox-$1^{+/+}$ recipients was similar when the reverse background strain combination (i.e., B10.A donors transplanted into 129Sv × BALB/c recipients) was used (Fig. 2 B). Thus the "protection" conferred by Hmox-1 cannot be ascribed to the reversal of donor and recipient strains, which in other model systems can affect the course of rejection despite identical allogeneic disparity (10). These data suggest that Hmox-1 expressed by graft epithelium, rather than by graft-infiltrating leukocytes, exerts the dominant influence on airway rejection.

To further delve into the pathway by which CO reduces graft luminal occlusion, a selective inhibitor of GC, 1H-[1,2,4]oxadiazolo[4,3,-a]quinoxalin-1-one (ODQ) was given to Hmox-$1^{+/+}$ allograft recipients during the period of CO inhalation. These data show that inhibition of GC during CO exposure did not interfere with the suppressive effect of exogenous CO inhalation on graft occlusion (35 ± 2% for CO + ODQ treatment in Hmox-$1^{+/+}$ allografts, 31 ± 3% for CO exposure alone; P = NS), indicating that CO elicits its beneficial effects through a cyclic cGMP-independent pathway.

Immunoreactivity for Hmox-1, CD3, and iNOS in adjacent sections

The prominent mononuclear cell infiltrate that was observed was comprised primarily of T cells, as determined by immunohistochemical analysis for the pan–T cell marker CD3 (Fig. 3, a–f). Quantitation of CD3 positive cells in histological sections reveals an approximate doubling of the number of CD3 positive cells in Hmox-$1^{-/-}$ allografts compared with Hmox-$1^{+/+}$ allografts. Immunoreactivity for Hmox-1 in epithelial cells was detected strongly in CoPP-treated Hmox-$1^{+/+}$ allografts (Fig. 3 i) and moderately in Hmox-$1^{+/+}$ allografts (Fig. 3 h), but was hardly detectable in Hmox-$1^{-/-}$ allografts (Fig. 3 k). Some graft-infiltrating cells (lymphocytic predominance) express Hmox-1 in each allograft (Fig. 3, h–l). These data indicate that epithelial cells in allografts represent a major source of Hmox-1 expression. iNOS expression was localized in both epithelial cells and infiltrating cells (Fig. 3, m–r), which were partly recognized as $CD3^+$ lymphocytes detected in adjacent serial sections. Immunoreactivity for iNOS was strongly expressed in graft-infiltrating lymphocytes in Hmox-$1^{-/-}$ allografts (Fig. 3 q). CO exposure for 2 wk prevented up-regulation of iNOS in both Hmox-$1^{+/+}$ (Fig. 3 p) and Hmox-$1^{-/-}$ allografts (Fig. 3 r).

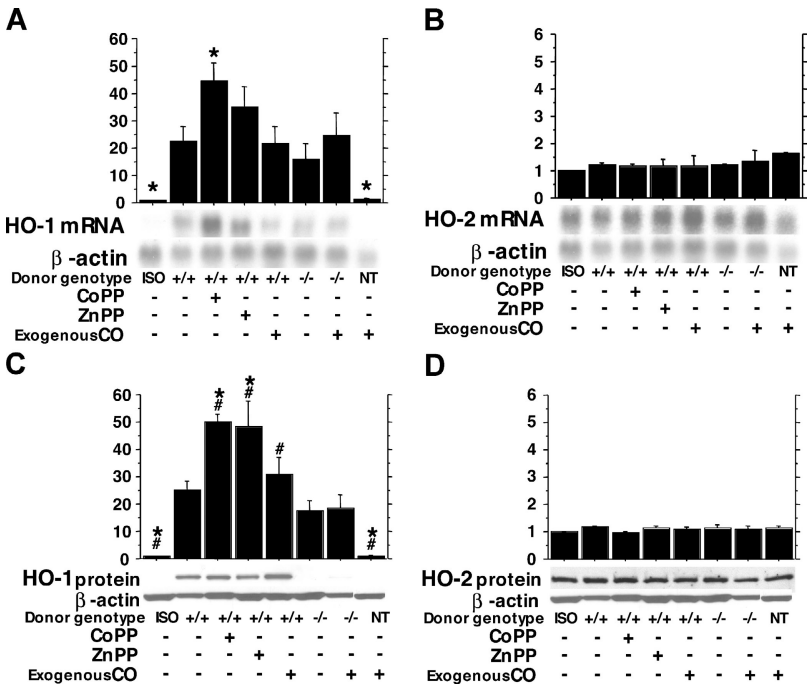

Figure 4. Northern and Western blots showing levels of Hmox-1 (HO-1) and Hmox-2 (HO-2) in grafts. All recipients were Hmox-$1^{+/+}$ (donor genotypes are indicated in the figure). (A and C) Effect of CoPP, ZnPP, or CO inhalation on Hmox-1 mRNA ($n = 4$) and protein ($n = 5$) levels. (B and D) The same effects for Hmox-2 mRNA and protein. The representative blots and treatment regimen are indicated under the bars, which display the densitometric mean ± SEM relative to β-actin (normalized to isograft values). The y axis indicates the fold increase versus isograft. ISO, isografts; NT, nontransplanted recipients; *, $P < 0.05$ versus Hmox-$1^{+/+}$; #, $P < 0.05$ versus Hmox-$1^{-/-}$ allografts.

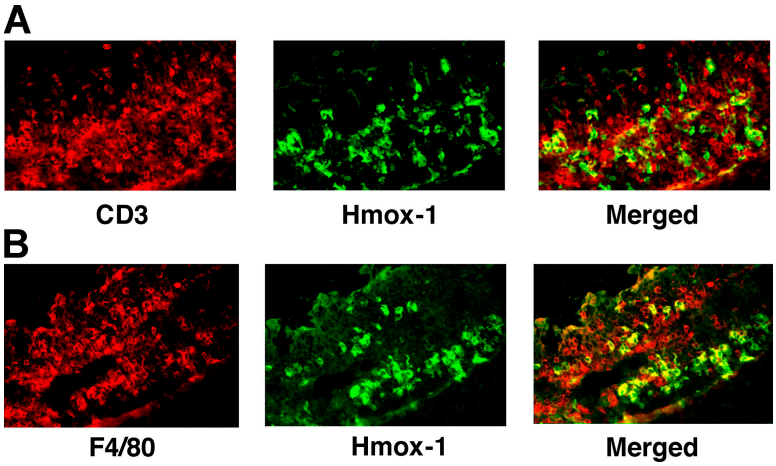

Figure 5. Confocal microscopic assessment of specific leukocyte populations expressing Hmox-1. Colocalization of Hmox-1 and CD3 (A) and Hmox-1 and F4/80 (marker of macrophages; panel B) in Hmox-$1^{-/-}$ allografts. $CD3^+$ T cells and $F4/80^+$ macrophages were labeled with FITC and detected as a green emission. Hmox-1^+ cells were labeled with PE and detected as a red emission. Sites of colocalization are indicated as a yellow emission.

Induced levels of mRNA and protein for Hmox-1 and Hmox-2 in airway grafts

To quantify the levels of both mRNA and protein for Hmox-1 and Hmox-2 induction in airway grafts, Northern and Western blots were performed on graft tissue extracts. Normalized Hmox-1 levels for both mRNA (Fig. 4 A) and protein (Fig. 4 C) were significantly increased in Hmox-$1^{+/+}$ allografts compared with isografts (22-fold and 25-fold increases, respectively; $P < 0.05$ for both comparisons). Levels of both Hmox-1 mRNA and protein in Hmox-$1^{+/+}$ allografts were up-regulated by CoPP treatment (both twofold increases; $P < 0.05$). Paradoxically, treatment with ZnPP also caused an increase in levels of Hmox-1 mRNA and protein in Hmox-$1^{+/+}$ allografts (1.6-fold and 2-fold increases, respectively; $P < 0.05$ for protein levels; reference 11). No significant increase was seen after exogenous CO exposure. In Hmox-$1^{-/-}$ allografts, the expression of both Hmox-1 mRNA and protein in Hmox-$1^{-/-}$ allografts was also increased compared with that seen in isografts (16-fold and 17-fold increases, respectively; $P < 0.05$ for protein levels). Colocalization experiments confirm that this is primarily secondary to Hmox-1 expression in the infiltrating cells, rather than allograft material (Fig. 5, A and B). Graft expression of Hmox-2 mRNA (Fig. 4 B) and protein (Fig. 4 D) was detected at the same low levels in all groups. There was no effect of CO exposure on expression of Hmox-1 and Hmox-2 in fresh tracheal tissue taken from nontransplanted mice.

Hmox activity and blood levels of COHb

Hmox enzymatic activity was measured based on the stoichiometric production of biliverdin and CO from heme substrate. After enzymatic reduction of biliverdin to bilirubin, tissue concentrations of bilirubin measured in Hmox-$1^{+/+}$ allografts were found to be 2.7-fold higher than those in isografts (Fig. 6 A). Compared with Hmox-$1^{+/+}$ allografts, the levels of Hmox activity were substantially increased by CoPP treatment (3.5-fold increase; $P < 0.05$), but reduced (1.7-fold decrease) by Hmox-1 gene deficiency (Hmox-$1^{-/-}$ allografts). Exogenous CO inhalation did not affect the enzymatic activity. Blood levels of COHb measured at the time of death were significantly ($P < 0.05$) increased only when CoPP was given to mice (Fig. 6 B).

Effect of exogenous CO/NO exposure on cGMP levels in tracheal tissue

cGMP levels in nontransplanted native trachea were significantly ($P < 0.05$) elevated after either 1 d (10-fold increase) or 2 wk of 20 ppm NO exposure (an 8-fold increase). CO exposure (250 ppm) almost doubled cGMP levels at 1 d (P = NS), although cGMP levels returned to baseline levels after 2 wk (Fig. 6 C).

Effect of Hmox-1 induction and exogenous CO exposure on iNOS expression

Because iNOS expression has been causally implicated in the outcome of graft rejection, mRNA (Fig. 7 A) and protein (Fig. 7 B) levels in grafts were quantified. Both iNOS mRNA and protein levels were significantly increased in Hmox-$1^{+/+}$ allografts compared with isografts (14-fold and 19-fold increases, respectively; $P < 0.05$ for each comparison). Compared with Hmox-$1^{+/+}$ allografts, iNOS up-regulation was detected in both Hmox-$1^{-/-}$ allografts (1.7-fold increase for message and 2-fold increase for protein levels; $P < 0.05$ for protein levels) and ZnPP-treated Hmox-$1^{+/+}$ allografts (1.3-fold increase for protein levels). CoPP treatment in Hmox-$1^{+/+}$ allografts, however, suppressed iNOS induction (1.9-fold decrease for mRNA, P = NS; 2-fold decrease for protein levels, $P < 0.05$) versus Hmox-$1^{+/+}$ allografts. iNOS levels in Hmox-$1^{-/-}$ allografts were also suppressed by exogenous CO exposure (2.3-fold decrease for

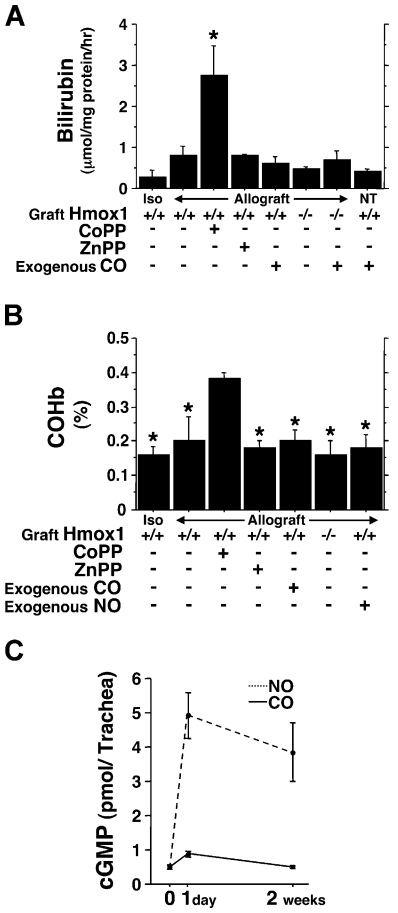

Figure 6. Hmox enzymatic activity in airway grafts. (A) Hmox enzyme activity was determined as the level of bilirubin generated in graft tissue ($n = 5$). *, $P < 0.05$ versus Hmox-$1^{+/+}$. Data are mean ± SEM. (B) Arterial blood levels of COHb were measured at the time of recipient sacrifice ($n = 5$). The donor Hmox-1 genotype and treatment regimen are indicated under each bar. ISO, isografts; NT, nontransplanted recipients; *, $P < 0.05$ versus CoPP-treated Hmox-$1^{+/+}$ allografts. Data are mean ± SEM. (C) Acute (1 d) and prolonged (2 wk) effects of CO/NO inhalation on cGMP levels in nontransplanted tracheal tissue ($n = 3$).

mRNA and 1.8-fold decrease for protein levels; $P < 0.05$ vs. Hmox-$1^{-/-}$ allografts for both comparisons). There was no effect of CO exposure on iNOS expression in fresh tracheal tissue taken from nontransplanted mice.

NO production assay

The levels of stable oxidant byproducts of NO (NO_2^- and NO_3^-) in airway grafts were determined as the total concentration of nitrite after conversion of all the sample NO_3^- into NO_2^- using nitrate reductase (Fig. 7 C). Compared with isografts, increased levels of nitrite (5.3-fold; $P < 0.05$) were detected in Hmox-$1^{+/+}$ allografts. Nitrite levels were increased further after ZnPP treatment (twofold increase; $P < 0.05$ vs. Hmox-$1^{+/+}$ allografts) and even more significantly increased in Hmox-$1^{-/-}$ allografts (3.9-fold increase; $P < 0.05$ vs. Hmox-$1^{+/+}$ allografts). On the other hand, nitrite levels were reduced by either CoPP treatment (2.5-fold decrease) or exogenous CO exposure (2.8-fold decrease) compared with Hmox-$1^{+/+}$ allografts. Exposure of Hmox-$1^{-/-}$ allografts to inhaled CO also decreased NO production (2.2-fold decrease; $P < 0.05$ vs. Hmox-$1^{-/-}$ allografts).

Effect of Hmox-1 induction and exogenous CO inhalation on iNOS-specific NF-κB binding activity

The striking down-regulation of iNOS expression by CO, which may account for some of the biological potency of CO as an inhibitor of airway allograft rejection, led us to investigate whether CO affects transcriptional regulation of the *iNOS* gene in transplanted airway tissue. There are two

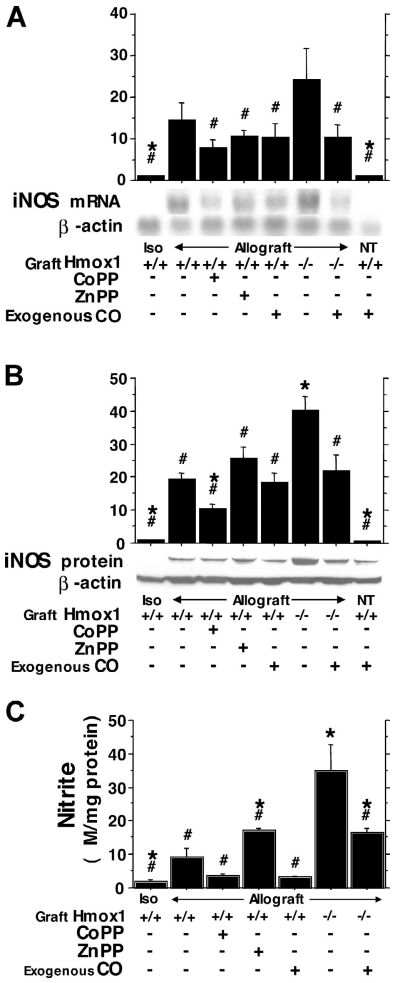

Figure 7. Effect of graft Hmox-1 genotype, treatment with CoPP, ZnPP, and CO on graft iNOS induction. (A and B) Analysis of iNOS mRNA and protein expression by Northern ($n = 4$) and Western ($n = 5$) blotting. Representative blots, corresponding donor Hmox-1 genotype, and treatment regimen are indicated under each bar. β-Actin was used to control for lane loading. The y axis indicates the fold increase versus isograft. (C) Total NO production (measured as nitrite in reduced samples) in airway grafts measured at 3 wk after transplantation ($n = 5$). ISO, isografts; NT, nontransplanted recipients. *, $P < 0.05$ versus Hmox-$1^{+/+}$; #, $P < 0.05$ versus Hmox-$1^{-/-}$ allografts. Data are mean ± SEM.

known NF-κB binding sites in the iNOS promoter region, one upstream (NF-κB*u*) and one downstream (NF-κB*d*). Electrophoretic mobility shift assay (EMSA) was performed to investigate the binding activity for each (Fig. 8 A, NF-κB*u,* and B, NF-κB*d*). Transplantation resulted in insubstantial changes in NF-κB*u* DNA binding activity in tissue taken from all conditions studied, suggesting minor or no involvement of this promoter site in *iNOS* gene regulation in the setting of airway transplantation. In contrast, NF-κB*d* was activated in the setting of allograft transplantation. In allografts in which Hmox activity was pharmacologically (by ZnPP) or genetically reduced (Hmox-$1^{-/-}$), there was clear up-regulation of formation of binding complexes in the downstream NF-κB site in the iNOS promoter. On the other hand, allografts in which Hmox-1 was pharmacologically up-regulated (with CoPP) or which had been treated with 250 ppm of chronic exogenous CO for 2 wk showed substantially less NF-κB*d* activation. No binding complexes (for either NF-κB*u* or NF-κB*d*) were detected in untreated isografts, nor in tracheas from nontransplanted control mice exposed to CO. Specificity of these results was demonstrated by supershift experiments. The binding complex was blocked and supershifted by antibody to p65, an NF-κB/Rel family member, using nuclear extracts from Hmox-$1^{-/-}$ allografts (Fig. 8 C). A similar supershift was seen when a combination of anti-p50 and -p65 was used. The binding specificity of the NF-κB*d* complex was further ascertained by competition with unlabeled oligonucleotides. Furthermore, three-color fluorescent immunostaining demonstrated that immunoreactivity for p65 (red) was mainly detected in nuclei (blue) of $CD3^+$ T lymphocytes (green) infiltrating Hmox-$1^{-/-}$ allografts (Fig. 8 D). Collectively, these findings suggest that activation of Hmox-1 in allografts reduces the formation of a sequence-specific NF-κB*d* complex comprised of mainly p65 homodimers (12) in allograft tissue. Exposure of recipient mice to CO can completely substitute for this inhibitory effect of activated Hmox-1 in allografts.

IL-1β expression and localization

IL-1β levels in grafts were determined by Western blot analysis (Fig. 9 A). Compared with isografts, protein levels of IL-1β in Hmox-$1^{+/+}$ allografts were significantly up-regulated (15-fold increase; $P < 0.05$). Although neither administration of the Hmox inducer CoPP nor exogenous CO exposure affected IL-1β expression in Hmox-$1^{+/+}$ allografts, IL-1β was strongly induced in the setting of Hmox-1 gene deficiency (2.5-fold increase; $P < 0.05$ vs. Hmox-$1^{+/+}$ allografts). Chronic CO treatment, however, strongly suppressed IL-1β induction in Hmox-$1^{-/-}$ allografts (2.8-fold decrease; $P < 0.05$ vs. Hmox-$1^{-/-}$ allografts). Localization of IL-1β was determined using a digital deconvolution system. IL-1β expression (red) was mainly localized in epithe-

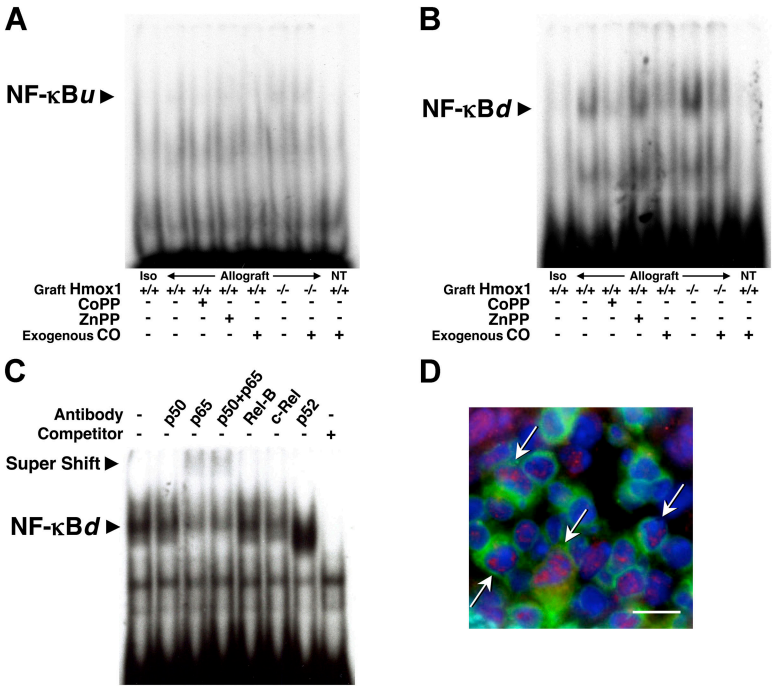

Figure 8. NF-κB binding activity in both upstream (NF-κB*u*) and downstream (NF-κB*d*) regions of the iNOS promoter by EMSA. (A and B) Binding activity was detected on NF-κB*d* but not NF-κB*u*. (C) Supershift assay using nuclear extracts prepared from Hmox-$1^{-/-}$ allografts. Extracts were incubated with or without the indicated antibodies or a 50-fold molar excess of unlabeled oligonucleotide probe as a competitor. The donor Hmox-1 genotype and treatment regimen are indicated under each lane. ISO, isografts; NT, nontransplanted recipients. (D) Intracellular expression of p65 identified as a red emission after the application of an excitation wavelength of 594 nm. $CD3^+$ T cells were labeled with FITC and detected as a green emission; nuclei (counterstained with DAPI) are identified by the blue emission spectra. Sites of colocalization are indicated by arrows. Bar, 5 μm.

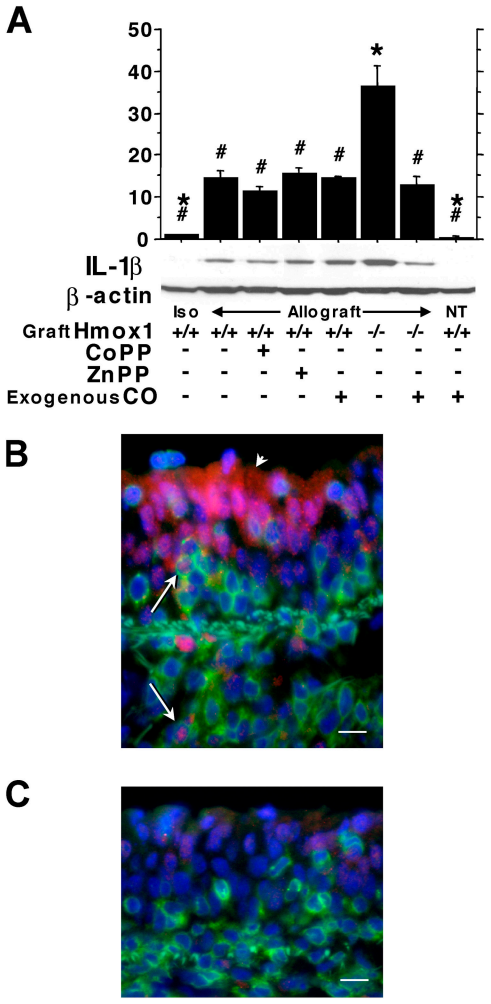

Figure 9. Effect of graft Hmox-1 genotype, treatment with CoPP, ZnPP, and CO inhalation on graft IL-1β induction. (A) Analysis of IL-1β protein expression by Western blotting ($n = 5$). Representative blots, corresponding donor Hmox-1 genotype, and treatment regimen are indicated under each bar. β-Actin was used to control for lane loading. ISO, isografts; NT, nontransplanted recipients; *, $P < 0.05$ versus Hmox-$1^{+/+}$ allografts; #, $P < 0.05$ versus Hmox-$1^{-/-}$ allografts. (B) Intracellular expression of IL-1β (identified as the red emission) is mainly detected in epithelial cells (arrowhead) of a representative section taken from Hmox-$1^{-/-}$ allografts. $CD3^+$ T cells labeled with FITC (detected as the green emission) also have some expression of IL-1β (arrows). (C) Exogenous CO treatment reduced IL-1β expression in epithelial cells of Hmox-$1^{-/-}$ allografts. Bar, 5 μm.

lial lining cells in Hmox-$1^{-/-}$ allografts, but also detected in $CD3^+$ T-lymphocytes (Fig. 9 B, green). Histological data using this technique show that exogenous CO exposure reduced the expression of IL-1β in epithelial cells (Fig. 9 C), in excellent concordance with the Western blot data.

DISCUSSION

NO and CO, both diatomic gases that bind to heme and activate GC, have entirely opposite effects in the setting of airway transplantation. When acutely inhaled after isogeneic rat lung transplantation, inhaled NO was without effect on vascular resistance, gas exchange, leukocyte infiltration, or recipient survival (13). When exogenous NO is inhaled for 2 wk at a dose of 20 ppm, there is essentially no effect on rejection in a rat model of lung allograft transplantation (14). In the present studies, 20 ppm of inhaled NO given for 2 wk in a murine air-flow permissive model of airway transplantation not only fails to reduce allograft airway occlusion but actually increases it slightly. Endogenous expression of iNOS is frankly pathological in this same murine model of airway transplantation (2). iNOS expression increases local expression of MIP-1α and RANTES, exacerbates development of a $CD3^+CD8^+$ T cell lymphocytic bronchitis, and ultimately contributes to airway luminal obliteration (2). These data are in sharp contrast to the role of endogenous Hmox expression and local CO generation, or the effect of exogenous CO administration. In the current experiments, both endogenous and exogenous CO were shown to have a remarkable salutary effect on the transplanted airway, reducing expression of inflammatory cytokines, leukocyte traffic, and eventual luminal obliteration.

Several lines of evidence point to the fact that the antirejection effects of CO are sGC independent. Even though inhaled doses of CO (250 ppm) and NO (20 ppm) were chosen for study based on theoretically similar levels of sGC stimulation (CO induces a 4.4-fold activation of purified sGC vs. a 130-fold activation of the enzyme by NO), only inhaled CO but not inhaled NO had a protective effect. Perhaps the strongest evidence comes from experiments in which pharmacological inhibition of GC with ODQ did not abrogate the beneficial effects of CO. Other authors (15–17) have shown that certain effects of CO, such as its antiapoptotic effects on endothelial cells, are cGMP independent. In that work, activation of p38 mitogen-activated protein kinase was shown to underlie the antiapoptotic effects of CO. It is possible that similar mechanisms might apply in our model of OB. To investigate the potential link between CO and NO, the effect of CO on iNOS induction was explored.

Inhalation of CO results in marked suppression of NF-κB activation, an upstream transcriptional event that triggers several proinflammatory processes. NF-κB is an important acute phase immune regulator, as well as a regulator for development of T lineage cells (18) and T cell–dependent immune responses (19). NF-κB also has an important facilitory role in allograft rejection, including expression of chemokine and cytokine production (20). NF-κB is also a potent regulator of iNOS transcription (21). Of the two putative NF-κB regulatory binding sites in the iNOS promoter region, NF-κB*d* appears to be more importantly involved in induction of the *iNOS* gene than NF-κB*u* in LPS-stimulated macrophages (21) or in tracheal allografts (Fig. 8 B). Our data strongly support the hypothesis that Hmox-1–derived CO is responsible for suppressing NF-κB activation, thereby reducing iNOS gene transcription. Superinduction of Hmox-1 with CoPP treatment was associated with a profound reduction in NF-κB/DNA binding in wild-type allograft nuclear extracts. The suppressive effect of Hmox-1

on *iNOS* gene transcription is further demonstrated by the increased nuclear binding activity of the downstream site of NF-κB in Hmox-1$^{-/-}$ allografts and by the remarkable induction of iNOS mRNA and protein detected in this same group. Furthermore, our data suggest that CO is directly responsible for the Hmox-1–mediated suppression of iNOS, because exogenous CO inhalation decreased expression of a DNA binding protein corresponding to NF-κB*d* on EMSA and also decreased iNOS mRNA and protein expression. This does not preclude obligatory or secondary involvement of other signaling cascades, such as mitogen-activated protein kinase cascades, but this represents an opportunity for future investigation. Our data support the hypothesis that CO exerts its beneficial effects on the transplanted allogeneic airway by suppressing NF-κB activation, reducing iNOS induction, and, thus, attenuating the alloimmune response (2).

iNOS expression has been described as a deteriorative mediator in chronic rejection after lung transplantation (22). This damaging effect of iNOS may involve a peroxynitrite intermediary, as nitrotyrosine staining provides evidence of the reaction of NO with superoxide anion, and there is abundant data to support the toxicity of peroxynitrite (23). The increased presence of iNOS in allografts, especially leukocyte-derived iNOS rather than epithelium derived iNOS, appears to be most responsible for OB (2). We showed that expression of iNOS and generation of NO product in Hmox-1$^{+/+}$ allografts were enhanced by graft Hmox-1 deficiency, leading to promotion of the rejection process, whereas either activation of Hmox-1 in Hmox-1$^{+/+}$ allografts or exogenous CO inhalation in both Hmox-1$^{+/+}$ and Hmox-1$^{-/-}$ allografts down-regulated iNOS expression, resulting in improvement of graft luminal narrowing. A further suppressive effect for luminal occlusion was not seen by combined treatment of CO exposure and pharmacological iNOS inhibition with L-NIL during the early postoperative period, suggesting that exogenous CO may abrogate the involvement of iNOS in the process of allograft rejection. The diminution of nitrite likely reflects a global reduction in iNOS activity, which might be secondary to an interaction of CO with the heme in iNOS. An in vitro study (24) also supports our data, in that it reports that CO, but not bilirubin treatment, reduced LPS-induced iNOS expression and NO production.

The tremendous disparity between the data with inhaled NO (harmful with chronic inhalation) and inhaled CO (beneficial with chronic inhalation) do not imply that low doses of inhaled NO are useless in the acute lung transplant setting. When given to the pulmonary donor before lung harvest, inhaled NO blunts the decline in tissue cGMP levels and improves vascular function after lung transplantation in an isogeneic rat lung transplant model (13). When administered to patients after lung transplantation, inhalation of low levels (<80 ppm) of NO acts as a pulmonary vasodilator and platelet inhibitor that ameliorates early graft dysfunction (9). The failure of the sGC blockade to detract from the beneficial effect of long-term inhaled CO, as well as other evidence cited above, suggests that chronic CO does not work through a cGMP-based mechanism. Although there are several potential cGMP-independent mechanisms by which CO might exert its antirejection effects in airways, such as by modulating the activity of p38 (7) or ERK 1/2 (25) mitogen-activated protein kinase pathways, our data point to the strong possibility of an inhibitory effect on NF-κB activation, iNOS up-regulation, and cytokine induction through the cGMP-independent pathway.

Although alloimmune effector cells access the graft abluminally, it is clear that gases flowing over the airway luminal surface can fundamentally alter the biological properties of the graft and its infiltrating cells. We show that induction of Hmox-1 expression with CoPP increases endogenous CO generation, as evidenced by increased levels of COHb in arterial blood from CoPP-treated recipients. The contribution of Hmox-1 overexpression in Hmox-1$^{+/+}$ allografts, which was strongly protective against airway obliteration, could be completely replicated by exogenous CO inhalation in Hmox-1$^{-/-}$ allografts. Lack of the *Hmox-1* gene, or Hmox blockade with ZnPP, exacerbated allograft rejection and resulted in an increase of luminal narrowing, which was also suppressed by exposure of CO. The pharmacological inhibition of Hmox activity using ZnPP did not show the same exacerbation of luminal obliteration as seen in as Hmox-1$^{-/-}$ allografts. This might be because of the lack of specificity of ZnPP (11). It has also been reported that some metalloporphyrins, including ZnPP, can induce transcription of Hmox-1 (11). These data implicate CO generation as the dominant protective effector mechanism elicited by Hmox-1 expression in airway allograft rejection. Even though cytoprotective effects elicited by another catalytic byproduct of heme degradation (biliverdin) or subsequent bilirubin and ferritin formation might contribute to protection by antioxidant or other properties, the current findings suggest that the preeminent role for CO formation by Hmox-1 is in the mitigation of acute-on-chronic airway rejection.

If endogenous Hmox-1 expression increases secondary to the transplantation procedure, and if Hmox-1 is protective, one may wonder why, in Hmox-1$^{+/+}$ allografts, rejection develops at all. Our data here, as well as elsewhere in unrelated model systems, show that endogenous expression of Hmox-1 is protective only to a point; overexpression studies (using a chemical inducer [26, 27] or a transgene [27, 28]) reveal consistent ability to augment this endogenous protective mechanism. In our experiments, the protective effects of Hmox-1 against allograft luminal occlusion are maximal when the gene is overexpressed. This protection is not limited only to increased patency of the airway lumen, but also to reduced local proinflammatory cytokine expression and reduced recruitment of cytoeffector leukocyte populations. These other features may in fact contribute to the ultimate beneficial effects that are observed with Hmox-1 overexpression or CO inhalation.

Our previous study (2) indicated that iNOS expression in recruited cytoeffector lymphocytes correlated strongly

with the occurrence and severity of graft rejection. However, local epithelial expression of iNOS did not play a role in this process, as $iNOS^{-/-}$ airway allografts placed in $iNOS^{+/+}$ recipients developed the same amount of disease as $iNOS^{+/+}$ grafts placed in $iNOS^{+/+}$ recipients. This is in striking contrast to the Hmox-1 data presented here, in which local expression of Hmox-1 is shown to be of prime importance in suppressing airway rejection. The relative contribution of airway epithelial Hmox-1 expression versus Hmox-1 expression in recipient graft-infiltrating leukocytes was ascertained by transplanting $Hmox\text{-}1^{+/+}$ airway grafts into allogeneic $Hmox\text{-}1^{-/-}$ recipients or by transplanting the reverse combination ($Hmox\text{-}1^{-/-}$ donor tissue into $Hmox\text{-}1^{+/+}$ recipients). Results demonstrated significantly increased ($P < 0.05$) allograft luminal occlusion when Hmox-1 was absent in donor but not recipient tissue, implicating a critical contribution of epithelium-derived Hmox-1, rather than infiltrating leukocyte-derived Hmox-1, in suppressing development of airway rejection. These results also suggest that inhalation of exogenous CO, which is likely to act most immediately on epithelial cells into which it first comes into contact, may be particularly efficacious in the setting of lung transplantation.

Collectively, the current results suggest a new paradigm for an endogenous protective mechanism against airway rejection (epithelium-derived Hmox-1 and CO), which can be bolstered by chronic inhalation of exogenous CO gas. It is intriguing that another diatomic gas, NO, which even more potently stimulates GC, has a facilitating effect on airway rejection, either when expressed endogenously (via iNOS) or when inhaled. The immunosuppressant effects of CO in this model of airway rejection are not only GC independent, but are associated with reduced NF-κB binding in the iNOS promoter and reduced up-regulation of iNOS. These data, therefore, highlight the negative reciprocal interactions between two quintessential biological diatomic gases (CO and NO) and the enzymes that produce them.

MATERIALS AND METHODS

Mice. B10.A ($H2^a$) mice were purchased from the Jackson Laboratories. For certain experiments, male $Hmox\text{-}1^{-/-}$ mice (129Sv × BALB/c background) were used (29) with $Hmox\text{-}1^{+/+}$ progeny serving as littermate controls. The genotype was confirmed by genomic PCR (30). All mice were between 7 and 15 wk old (25–30 g). Isogeneic tracheal transplants were performed using B10.A mice as both recipients and donors. Allogeneic (129Sv × BALB/c) tracheal grafts from wild-type ($Hmox\text{-}1^{+/+}$) or $Hmox\text{-}1^{-/-}$ donor mice were transplanted into wild-type (B10.A) recipient mice. To specifically determine the role of epithelial- versus leukocyte-derived Hmox-1, reverse donor/recipient transplantation experiments were performed using wild-type donor (B10.A) airway allografts transplanted into $Hmox\text{-}1^{+/+}$ or $Hmox\text{-}1^{-/-}$ recipients. All experiments were performed according to protocols approved by the Association for Assessment and Accreditation of Laboratory Animal Care guidelines.

Tracheal transplantation, immunosuppression, sample acquisition, and CO measurements. Experiments were performed in a recently described double-lumen airway transplant model for studying chronic airway rejection (2). In brief, donor mice were exsanguinated after anesthesia, and whole tracheas were harvested by transecting below the cricoid cartilage distal to the carinal bifurcation under sterile conditions. Recipient mice were similarly anesthetized, and whole tracheas were exposed. Distal (the sixth intercartilaginous space) and proximal (immediately subjacent to the cricoid cartilage area) orifices positioned on the recipient trachea were anastomosed with both ends of the tracheal graft.

All recipient animals received postoperative intramuscular immunosuppression (25 mg/kg/d cyclosporine; Bedford Laboratories) for 2 wk, to model acute-on-chronic airway rejection, and antibiotics (20 mg/kg/d cefazolin sodium; Apothecon) for 3 d. All recipient animals survived and were killed at 3 wk after transplantation. The percent COHb content of 100 μl of arterial blood was determined using a CO-oximeter (Nova; Waltham) at the time of death. Tracheal grafts were harvested and snap frozen or embedded en bloc with the native tracheas in Tissue Freezing Medium (Triangle Biomedical Sciences) in a cryomold in liquid nitrogen and stored at −80°C until the time of analysis.

Pharmacological regulation of Hmox-1 induction. To induce Hmox-1 expression during the rejection process, wild-type donor or recipient mice were given 5 mg/kg CoPP (Frontier Scientific) i.p. at days 5 and 1 before transplantation to the donor and days 0 and 5 after transplantation to the recipient (26). The effect of CoPP on endogenous CO production was confirmed by measurements of graft Hmox-1 expression and levels of COHb in arterial blood at the time of death, as described in the previous section. Hmox activity was inhibited using 20 mg/kg ZnPP (Frontier Scientific), a competitive inhibitor, administered i.p. (27) at the same times as described for CoPP.

Exogenous CO/NO exposure. Mice that were exposed to CO or NO (or controlled room air exposure) were treated as follows. Cages were placed in a lucite exposure chamber (30) immediately after tracheal transplantation and exposed to either 250 ppm CO (balanced with air) or 20 ppm NO (blended with air just before exposure; TechAir). These concentrations of CO (7, 24, 26, 31) or NO (32) were based on previous reports of their use in different model systems. CO levels in the chamber were maintained at 250 ppm monitored with a CO detector (PhD Ultra; Biosystems). NO level was maintained at 20 ppm, keeping the NO_2 level <5 ppm by flowing freshly blended gas into the chamber and monitoring with a detector (Q-RAE; Geotech). Exposure was initiated immediately after completion of the surgical procedure. Recipient mice were removed from the chamber for only the time required for the daily injection (immunosuppressor or pharmacological inhibitor). After 2 wk, cages were placed in room air for the remaining 1 wk until death. Nontransplanted mice were killed immediately after 2 wk of CO or NO exposure, at which time blood samples were collected from the left ventricle for measurement of COHb levels. In nontransplanted mice, native tracheal segments were also harvested in order to determine the possible effects of these gases on the tissue levels of cGMP (1 d or 2 wk of CO or NO exposure) or expression of Hmox-1, Hmox-2, iNOS, and IL-1β (2 wk of CO or NO exposure). For experiments to evaluate the effect of CO administration to the donor, donor mice were exposed to CO over 24 h before graft harvesting, and the grafts were transplanted into recipient mice without further CO exposure.

Pharmacological inhibition for cGMP and iNOS induction. In certain experiments coincident with the placement of $Hmox\text{-}1^{+/+}$ allograft recipient animals in the CO chamber, mice were given a daily dose of 5 mg/kg ODQ intramuscularly (33) for 2 wk after transplantation. In experiments designed to study the combined effects of CO exposure and iNOS suppression, both $Hmox\text{-}1^{+/+}$ and $Hmox\text{-}1^{-/-}$ allograft-recipient mice were placed in the CO chamber for 2 wk, during which time they were given 5 mg/kg of the selective iNOS inhibitor L-NIL (Cayman Chemical) i.p. daily, a treatment that was continued into the third week after transplantation, as previously reported (2).

Histopathological evaluation. 5-μm-thick frozen sections were cut and placed on glass slides (Fisher Scientific), after which sections were air dried and fixed for 15 min in acetone at 4°C. Histochemical staining was per-

formed for elastin (Accustain; Sigma-Aldrich) in order to determine graft luminal occlusion. Immunostaining was also performed using serial adjacent sections from each group, with primary antibodies directed against a pan–T cell marker (hamster anti–mouse CD3; BD Biosciences), Hmox-1, Hmox-2 (rat anti–mouse Hmox-1 and rat anti–mouse Hmox-2; StressGen Biotechnologies), or iNOS (rabbit anti–mouse iNOS; Transduction Laboratories).

Morphometric measurements of cross-sectional areas were performed by blindly tracing both epithelial and subepithelial areas using a computer-assisted image analysis system (AxoCamHR; Carl Zeiss MicroImaging, Inc.).

Localization of sites of intracellular NF-κB expression was determined with a digital deconvolution system (Isee Imaging Systems) using a fluorescence microscope (Axiovert S100; Carl Zeiss MicroImaging, Inc.). A series of images was generated from multiparameter (three-color) immunofluorescent staining techniques. After blocking nonspecific binding and FcRs with normal goat serum and the FcR blocker anti-2.4G2 (BD Biosciences), $CD3^+$ T cells were detected by FITC-conjugated antibodies (anti–mouse CD3; BD Biosciences). Sections were then fixed and permeabilized using a Cytofix/CytopermTM kit (BD Biosciences). Each section was then incubated with rabbit anti–mouse p65 (Santa Cruz Biotechnology, Inc.), rabbit anti–mouse IL-1β (Cell Sciences), or rabbit IgG (as a negative control) at 4°C for 30 min in the dark. Intracellular NF-κB or cytokine (IL-1β) were identified by incubating the sections with a fluorescent secondary antibody (AlexaFluor 594 goat anti–rabbit IgG; Molecular Probes) followed by a nuclear counterstain (DAPI).

Northern blotting. The cDNA probe for the detection of iNOS mRNA was prepared as described previously (2). RT-PCR was performed to make Hmox-1 and Hmox-2 cDNA probes. Primers for mouse Hmox-1 and Hmox-2 were directed at regions 125/1323 (available from GenBank/EMBL/DDBJ under accession no. NM 010442) and 139/1137 (available from GenBank/EMBL/DDBJ under accession no. XM 147238) of each gene, respectively, producing a 1,198- and a 998-bp product for each respective reaction. The forward and reverse primers sequences for Hmox-1 were 5′-GTGATGGAGCGTCCACAGCCCGACA-3′ and 5′-AAAGTGGCCATGGCACTGGGGGACA-3′. The sequences for Hmox-2 were 5′-GGGCAGCACAAACTACTCAGCCACA-3′ and 5′-GGGATAGAACAGGTCACTTGGGGTA-3′. The RT-PCR product mixture was extracted and inserted into pCRII Vector using the TA cloning method (Invitrogen). The cDNA expression plasmid was confirmed by enzyme cut and was also sequenced (ABI Prism 310; PE Biosystems). Total RNA was isolated from each tracheal graft after tissue homogenization, and 15 μg of each was electrophoresed and transferred to nitrocellulose membranes. Specific mRNAs were identified by hybridization to the indicated probes labeled with α-[^{32}P]dCTP. Normalized absorption values were obtained by densitometry scanning of labeled bands (National Institutes Health Image 1.62; National Institutes of Health), including β-actin bands. Expression of each band was normalized with its corresponding β-actin band, and this ratio was then normalized with that of the isograft sample for each experiment.

Western blotting. SDS-PAGE gels were loaded with samples of tissue protein (30 μg/lane), subjected to electrophoresis, transferred electrophoretically to nitrocellulose membranes, and reacted with the following primary antibodies: anti–Hmox-1, Hmox-2, and iNOS (the same primary antibodies as in immunohistochemistry), and rabbit anti–mouse IL-1β (Cell Sciences). Secondary detection of primary antibody localization was accomplished using horseradish peroxidase–conjugated antibodies directed against the appropriate species (Sigma-Aldrich). Bands were revealed using the chemiluminsecent method of detection on X-ray film (GE Healthcare). Expression of each band was normalized to its corresponding β-actin band (mouse anti–β-actin; Sigma-Aldrich), and this ratio was then normalized with that of the isograft sample for each experiment.

Measurement of Hmox activity. Hmox enzymatic activity was determined by measuring bilirubin generated in transplanted airway grafts (34). Tissue was homogenized in protein extract solution containing 0.6% NP-40 (Roche), 150 mM NaCl, 10 mM Hepes, pH 7.9, 1 mM EDTA, and 0.5 mM PMSF (Sigma-Aldrich) on ice, and centrifuged at 13,000 *g* for 10 min at 4°C. After determination of protein levels, measured using the Bradford method (Bio-Rad Laboratories), supernatants were incubated for 1 h at 37°C in the dark with the 200-μl reaction mixture containing mouse liver cytosol (1 mg of protein), 50 μM hemin, 1 mM NADPH, 2 mM glucose 6-phosphate, and 0.2 U glucose-6-phosphate dehydrogenase (Sigma-Aldrich) in 0.1 M potassium phosphate buffer, pH 7.4. Bilirubin produced in this reaction was measured spectrophotometrically (ΔOD at 464–530 nm; extinction coefficient, 40 mM/liter/cm for bilirubin). Hmox activity is expressed as micromoles of bilirubin formed per milligram of protein per hour (μmol/mg protein/hr). The background activity of the reaction mixture with liver cytosolic extract alone (without tracheal tissue homogenate) was subtracted from each sample reaction to determine the specific activity of the added sample.

Measurement of NO production. To determine concentrations of the final products of NO in airway grafts, the total concentration of nitrite in the protein extracts of grafts was measured using an NO detection kit (StressGen Biotechnologies). Values were normalized per milligram of corresponding tissue protein (μM/mg protein).

Tracheal cGMP assay. To demonstrate the effect of exogenous CO or NO exposure on cGMP levels in tracheal tissue, enzyme immunoassays were performed using commercial kits (cGMP EIA Kit; Cayman Chemical). Whole tracheas from nontransplanted mice were homogenized in 200 μl of 5% TCA buffer. After centrifugation, supernatant fractions were extracted with water-saturated ether, followed by heating to remove the residual ether. Samples were diluted twice with phosphate buffer and assayed for cGMP content according to the manufacturer's instructions. Values are indicated as picomoles per trachea.

EMSA. There are two putative regulatory binding sites of NF-κB in the upstream (distal) and downstream (proximal) regions of the iNOS promoter (available from GenBank/EMBL/DDBJ under accession no. L09126; reference 21) recognized as NF-κB*u* (GGGATTTTCC; −971 to −962 bp) and NF-κB*d* (GGGACTCTCC; −85 to −76 bp). To generate oligonucleotide probes containing binding sites for NF-κB*u* and NF-κB*d*, consensus sequences (NF-κB*u*, 5′-TGCTAGGGGGATTTTCCCTCTCTCTGT-3′; NF-κB*d*, 5′ CCAACTGGGGACTCTCCCTTTGGGAACA-3′) were prepared by Invitrogen. Gel shift assays were performed on nuclear extracts prepared from tissue samples, as previously described (35). Probes were 5′-labeled with γ-[^{32}P]ATP (3,000 Ci/mmol) using T4 polynucleotide kinase (Promega). 5 μg of extracted nuclear proteins were incubated with 0.1 ng ^{32}P-labeled DNA for 20 min at room temperature in 10 μl binding buffer containing 1 μg poly(dI-dC). To characterize the proteins involved in the binding to the site of NF-κB, supershift assays were performed using 4 μg of one of the following antibodies: p50, p65, RelB, c-Rel, or p52 (Santa Cruz Biotechnology, Inc.). These antibodies were preincubated with the nuclear extract mixture for 60 min at room temperature before the binding reaction. The samples were electrophoresed on 6% nondenaturing polyacrylamide/bisacrylamide gels (DNA retardation gel; Invitrogen) at room temperature for 1 h at 100 V. Competition experiments were performed by adding a 100-fold molar excess of either unlabeled NF-κB*u* or NF-κB*d* probes.

Statistics. Data are expressed as mean ± SEM. All statistical comparisons were performed using a commercially available statistical package for the Macintosh personal computer (Stat View-J 5.0; SAS Institute). One-way analysis of variance and the Fisher's posthoc test were used to compare conditions between groups. Differences of $P < 0.05$ were considered significant.

We would like to thank Dr. Kim Olson and Dr. Hui Liao for expert technical advice.

This work was supported in part by the U.S. Public Health Service (grants HL55397 and HL60900).

David J. Pinsky is a consultant to Aga-Linde Healthcare. The authors have no other conflicting financial interests.

Submitted: 8 March 2005
Accepted: 13 April 2005

REFERENCES

1. Yousem, S.A., G.J. Berry, P.T. Cagle, D. Chamberlain, A.N.H. Husain, A. Marchevsky, N.P. Ohori, J. Ritter, S. Stewart, and H.D. Tazelaar. 1996. Revision of the 1990 working formulation for the classification of pulmonary allograft rejection: lung rejection study group. *J. Heart Lung Transplant.* 15:1–15.
2. Minamoto, K., and D. Pinsky. 2002. Recipient iNOS but not eNOS deficiency reduces luminal narrowing in tracheal allografts. *J. Exp. Med.* 196:1321–1333.
3. Lu, F., D.S. Zander, and G.A. Visner. 2002. Increased expression of heme oxygenase-1 in human lung transplantation. *J. Heart Lung Transplant.* 21:1120–1126.
4. Choi, A.M., and J. Alam. 1996. Heme oxygenase-1: function, regulation, and implication of a novel stress-inducible protein in oxidant-induced lung injury. *Am. J. Respir. Cell Mol. Biol.* 15:9–19.
5. Maines, M.D. 1997. The heme oxygenase system: a regulator of second messenger gases. *Annu. Rev. Pharmacol. Toxicol.* 37:517–554.
6. Willis, D., A.R. Moore, R. Frederick, and D.A. Willoughby. 1996. Heme oxygenase: a novel target for the modulation of the inflammatory response. *Nat. Med.* 2:87–90.
7. Otterbein, L., F. Bach, and J. Alam. 2000. Carbon monoxide has anti-inflammatory effects involving the mitogen-activated protein kinase pathway. *Nat. Med.* 6:422–428.
8. Kermarrec, N., P. Zunic, S. Beloucif, J. Benessiano, L. Drouet, and D. Payen. 1998. Impact of inhaled nitric oxide on platelet aggregation and fibrinolysis in rats with endotoxic lung injury. Role of cyclic guanosine 5′-monophosphate. *Am. J. Respir. Crit. Care Med.* 158:833–839.
9. Date, H., A.N. Triantafillou, E.P. Trulock, M.S. Pohl, J.D. Cooper, and G.A. Patterson. 1996. Inhaled nitric oxide reduces human lung allograft dysfunction. *J. Thorac. Cardiovasc. Surg.* 111:913–919.
10. Russell, P.S., C.M. Chase, H.J. Winn, and R.B. Colvin. 1994. Coronary atherosclerosis in transplanted mouse hearts. II. Importance of humoral immunity. *J. Immunol.* 152:5135–5141.
11. Hajdena-Dawson, M., W. Zhang, P.R. Contag, R.J. Wong, H.J. Vreman, D.K. Stevenson, and C.H. Contag. 2003. Effects of metalloporphyrins on heme oxygenase-1 transcription: correlative cell culture assays guide in vivo imaging. *Mol. Imaging.* 2:138–149.
12. Ganchi, P.A., S.C. Sun, W.C. Greene, and D.W. Ballard. 1993. A novel NF-kappa B complex containing p65 homodimers: implications for transcriptional control at the level of subunit dimerization. *Mol. Cell. Biol.* 13:7826–7835.
13. Naka, Y., D.K. Roy, A.J. Smerling, R.E. Michler, C.R. Smith, D.M. Stern, M.C. Oz, and D.J. Pinsky. 1995. Inhaled nitric oxide fails to confer the pulmonary protection provided by distal stimulation of the nitric oxide pathway at the level of cyclic guanosine monophosphate. *J. Thorac. Cardiovasc. Surg.* 110:1434–1441.
14. Shiraishi, T., K. Kawahara, T. Shirakusa, K. Okabayashi, S. Yoneda, and A. Iwasaki. 1998. Inhaled nitric oxide does not increase rat pulmonary allograft rejection. *J. Heart Lung Transplant.* 17:573–577.
15. Brouard, S., L.E. Otterbein, J. Anrather, E. Tobiasch, F.H. Bach, A.M.K. Choi, and M.P. Soares. 2000. Carbon monoxide generated by heme oxygenase 1 suppresses endothelial cell apoptosis. *J. Exp. Med.* 192:1015–1025.
16. Zhang, X., P. Shan, J. Alam, R.J. Davis, R.A. Flavell, and P.J. Lee. 2003. Carbon monoxide modulates Fas/Fas ligand, caspases, and Bcl-2 family proteins via the p38α mitogen-activated protein kinase pathway during ischemia-reperfusion lung injury. *J. Biol. Chem.* 278:22061–22070.
17. Pae, H.-O., G.-S. Oh, B.-M. Choi, S.-C. Chae, Y.-M. Kim, K.-R. Chung, and H.-T. Chung. 2004. Carbon monoxide produced by heme oxygenase–1 suppresses T cell proliferation via inhibition of IL-2 production. *J. Immunol.* 172:4744–4751.
18. Boothby, M., A. Mora, D. Scherer, J. Brockman, and D. Ballard. 1997. Perturbation of the T lymphocyte lineage mice expressing a constitutive repressor of nuclear factor (NF)-κB. *J. Exp. Med.* 185:1897–1907.
19. Attar, R., H. Macdonald-Bravo, C. Raventos-Suarez, S. Durham, and R. Bravo. 1998. Expression of constitutively active IkappaB beta in T cells of transgenic mice: persistent NF-kappaB activity is required for T-cell immune responses. *Mol. Cell. Biol.* 18:477–487.
20. Finn, P., J. Stone, M. Boothby, and D. Perkins. 2001. Inhibition of NF-kappaB-dependent T cell activation abrogates acute allograft rejection. *J. Immunol.* 167:5994–6001.
21. Xie, Q., Y. Kashiwabara, and C. Nathan. 1994. Role of transcription factor NF-kappaB/Rel in induction of nitric oxide synthase. *J. Biol. Chem.* 269:4705–4708.
22. Mason, N.A., D.R. Springall, A. Pomerance, T.J. Evans, M.H. Yacoub, and J.M. Polak. 1998. Expression of inducible nitric oxide synthase and formation of peroxynitrite in posttransplant obliterative bronchiolitis. *J. Heart Lung Transplant.* 17:710–714.
23. Mungrue, I.N., R. Gros, X. You, A. Pirani, A. Azad, T. Csont, R. Schulz, J. Butany, D.J. Stewart, and M. Husain. 2002. Cardiomyocyte overexpression of iNOS in mice results in peroxynitrite generation, heart block, and sudden death. *J. Clin. Invest.* 109:735–743.
24. Lee, T., and L. Chau. 2002. Heme oxygenase-1 mediates the anti-inflammatory effect of interleukin-10 in mice. *Nat. Med.* 8:240–246.
25. Song, R., R.S. Mahidhara, F. Liu, W. Ning, L.E. Otterbein, and A.M. Choi. 2002. Carbon monoxide inhibits human airway smooth muscle cell proliferation via mitogen-activated protein kinase pathway. *Am. J. Respir. Cell Mol. Biol.* 27:603–610.
26. Hancock, W., R. Buelow, M. Sayegh, and L. Turka. 1998. Antibody-induced transplant arteriosclerosis is prevented by graft expression of anti-oxidant and anti-apoptotic genes. *Nat. Med.* 4:1392–1396.
27. Otterbein, L.E., J.K. Kolls, L.L. Mantell, J.L. Cook, J. Alam, and A.M. Choi. 1999. Exogenous administration of heme oxygenase-1 by gene transfer provides protection against hyperoxia-induced lung injury. *J. Clin. Invest.* 103:1047–1054.
28. Amersi, F., R. Buelow, and H. Kato. 1999. Upregulation of heme oxygenase-1 protects genetically fat Zucker rat livers from ischemia/reperfusion injury. *J. Clin. Invest.* 104:1631–1639.
29. Yet, S.F., M.A. Perrella, M.D. Layne, C.M. Hsieh, K. Maemura, L. Kobzik, P. Wiesel, H. Christou, S. Kourembanas, and M.E. Lee. 1999. Hypoxia induces severe right ventricular dilatation and infarction in heme oxygenase-1 null mice. *J. Clin. Invest.* 103:R23–R29.
30. Fujita, T., K. Toda, A. Karimova, S.F. Yan, Y. Naka, S.F. Yet, and D.J. Pinsky. 2001. Paradoxical rescue from ischemic lung injury by inhaled carbon monoxide driven by derepression of fibrinolysis. *Nat. Med.* 7:598–604.
31. Chapman, J.T., L.E. Otterbein, J.A. Elias, and A.M. Choi. 2001. Carbon monoxide attenuates aeroallergen-induced inflammation in mice. *Am. J. Physiol. Lung Cell. Mol. Physiol.* 281:L209–L216.
32. Roberts, J.D., Jr., C.T. Roberts, R.C. Jones, W.M. Zapol, and K.D. Bloch. 1995. Continuous nitric oxide inhalation reduces pulmonary arterial structural changes, right ventricular hypertrophy, and growth retardation in the hypoxic newborn rat. *Circ. Res.* 76:215–222.
33. Shinmura, K., Y.T. Xuan, X.L. Tang, E. Kodani, H. Han, Y. Zhu, and R. Bolli. 2002. Inducible nitric oxide synthase modulates cyclooxygenase-2 activity in the heart of conscious rabbits during the late phase of ischemic preconditioning. *Circ. Res.* 90:602–608.
34. Sato, K., J. Balla, L. Otterbein, R.N. Smith, S. Brouard, Y. Lin, E. Csizmadia, J. Sevigny, S.C. Robson, G. Vercellotti, et al. 2001. Carbon monoxide generated by heme oxygenase-1 suppresses the rejection of mouse-to-rat cardiac transplants. *J. Immunol.* 166:4185–4194.
35. Matsukura, S., C. Stellato, J.R. Plitt, C. Bickel, K. Miura, S.N. Georas, V. Casolaro, and R.P. Schleimer. 1999. Activation of eotaxin gene transcription by NF-kappa B and STAT6 in human airway epithelial cells. *J. Immunol.* 163:6876–6883.
36. Wahl, C., S. Liptay, G. Adler, and R.M. Schmid. 1998. Sulfasalazine: a potent and specific inhibitor of nuclear factor kappa B. *J. Clin. Invest.* 101:1163–1174.
37. Pittet, J.F., L.N. Lu, D.G. Morris, K. Modelska, W.J. Welch, H.V. Carey, J. Roux, and M.A. Matthay. 2001. Reactive nitrogen species inhibit alveolar epithelial fluid transport after hemorrhagic shock in rats. *J. Immunol.* 166:6301–6310.